Thermal load minimisation of the frequency domain multiplexed readout for the Athena X-IFU instrument

J. van der Kuur*, L.G. Gottardi*, H.A. Akamatsu*, B.J. van Leeuwen*, R. den Hartog*, M.Kiviranta† B. Jackson‡
*SRON, Sorbonnelaan 2, 3584CA Utrecht, the Netherlands, Email: see http://www.sron.nl
†VTT, Tietotie 3, FIN-02150 Espoo, Finland
‡SRON, Landleven 12, 9747AD Groningen, the Netherlands

***Abstract*—The high sensitivity of cryogenic TES-based detectors opens new windows for astrophysical observations ranging from (far) infrared to X-rays. A number of operational and future space and ground-based instruments rely on cryogenic detectors to improve their performance with respect the capabilities of earlier technologies. To reach the required sensitivities, base temperatures as low as 50 mK are necessary, and stringent requirements on magnetic shielding, micro-vibrations, and temperature stability are applicable.**

To minimize the heat load and complexity of the instruments, efficient multiplexing schemes and low power amplifiers are needed. In addition, for space based cryogenic instruments mechanical launch loads and power consumption limitations constrain the available parameter space for engineering further.

This paper discusses the system design considerations which are applicable to optimise the multiplex factor within the boundary conditions as set by the space craft for the X-IFU instrument on the Athena observatory. More specifically, the interplay between the science requirements such as pixel dynamic range, pixel speed, and cross talk, and the space craft requirements such as the power dissipation budget, and available bandwidth will be discussed.

I. Introduction

An imaging array of TES-based micro-calorimeters operated at 50 mK will be used in the focal plane of the X-ray Integral Field Unit (X-IFU), which is one of the instruments on board of ESAs Athena X-ray space telescope to be launched in 2028. The X-IFU instrument will provide the capability of high resolution spectroscopy in the energy range between 0.2 and 12 keV in a field of view of 5'. This translates into an imaging array of 3840 pixels of 250×250 μm, with an energy resolution of $\Delta E < 2.5$ eV for photon energies below 7 keV. More extended descriptions of the instrument capability and the design considerations of the focal plane assembly have been published recently [1], [2].

As the X-IFU is a space-based instrument, the available resources in terms of cooling power, mass, and electrical power are very limited[3]. As a result, careful optimisation of the resource consumption is needed to make the instrument feasible. The two major sources of heat load on the 50 mK cryogenic stage are the suspension and the dissipation by the SQUID amplifiers[4]. The heat load of the suspension is driven by the suspended mass[5], [2], which in turn depends on the size of the suspended objects, and the shielding. The heat load of the SQUID amplifiers depends on the multiplexing factor, the total number of pixels, and the power dissipation per SQUID. In this paper we will focus on the rationale behind the required power dissipation of the SQUID amplifier chain, and possible optimisations to lower the thermal load on the cryogenic stages.

II. Multiplexed readout

Readout of TES-based detectors requires SQUIDs as first stage amplifiers, as no other amplifier can deliver the combination of a sufficiently low noise temperature of typically 10% of the operating temperature of the TES, and the low input impedance which is needed to fulfill the voltage bias condition of the TES.

Since the bandwidth of a SQUID amplifier is much larger than the bandwidth of a micro-calorimeter pixel, multiplexing techniques can be used to combine the signals of multiple pixels in such a way that they remain independent. The resulting combined signals can then be amplified by a single SQUID chain, so that the total number of required SQUID chains gets reduced by the multiplexing factor.

Multiplexing requires a set of independent carriers, on which the bandwidth limited signals of the independent pixels are mounted by means of modulation. The modulated signals can then be added and transported through a single channel or amplified by a single amplifier, without loss of information. There are several multiplexing versions for TES-based detector readout under development. The NIST group has pioneered the use of SQUIDs as modulating element with different sets of carrier functions, i.e. box car functions for time domain multiplexing (TDM)[6], Walsh functions for code domain multiplexing (CDM)[7], and sinusoidal micro waves for microwave multiplexing. Other groups have pioneered the use of the TES as modulator, by using the TES as amplitude modulator of a sinusoidal alternating bias current. In this way multiplexing in the frequency domain (FDM) is obtained[8], [9], [10], [11].

The baselined readout scheme for X-IFU is FDM[1] with a multiplex factor of $N_{\rm mux} = 40$, and 96 readout chains of the readout of 3840 pixels. Each pixel is bandwidth limited by an LC bandpass filter. A more elaborate design rationale can be

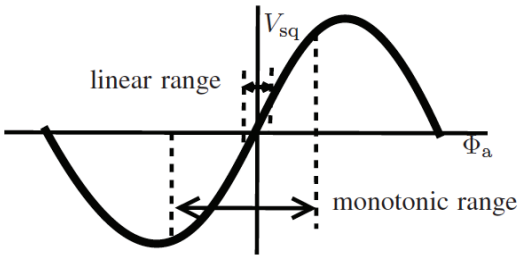

Fig. 1. Sketches of output voltage $V_{\rm sq}$ versus input flux $\Phi_{\rm a}(= M_{\rm in}I_{\rm in})$, for two input ranges: the full monotone range over which the SQUID shows a monotonic but non-linear transfer function, and the smaller linear range, over which the SQUID is both monotonic and linear.

found elsewhere[12]. For the latest status of the performance demonstration of FDM on micro-calorimeter pixels we refer to [11]. The energy (dynamic) range of the pixels is 0.2 - 12 keV, with an energy resolution of $\Delta E < 2.5$ eV @ 7 keV. The pixels will be operated with sinusoidal bias currents with frequencies between 1 and 5 MHz, with an inter pixel spacing of 100 kHz. To meet the dynamic range and bandwidth requirements set by the multiplexing factor and pixel dynamic range, a two-stage SQUID together with flux nulling baseband feedback is needed to be able to both drive the cables, and to boost the signal above the noise floor of the first stage low noise amplifier at room temperature[13], [12]. The first stage front-end SQUID resides at base temperature close to the detectors, and the second stage booster SQUID operates at 2 K where more cooling power is available.

III. Dynamic range requirements

The science requirements drive the required dynamic range and bandwidth of the readout chain, and therefore the power dissipation.

The dynamic range of a signal is defined as ratio between the largest and smallest value of the signal. For a TES-based microcalorimeter the largest signal is approximately equal to the bias current, and the smallest signal is set by root-mean-square (rms) value of the noise.

The signal dynamic range of a single X-IFU pixel follows from the saturation energy and the energy resolution requirement, so that $D \approx 2\sqrt{2\ln 2} \cdot 12$ keV$/2.5$ eV(FWHM) $=$ 41 dB as requirement, and 42 dB as goal.

The SQUID dynamic range is determined by the ratio between its usable flux range and the equivalent input rms flux noise. The flux dynamic range and the input current dynamic range are equal, as $\Phi_{\rm n} = M_{\rm in} i_{\rm n}$, with $M_{\rm in}$ the mutual inductance between the SQUID input coil and the SQUID loop inductance, and $i_{\rm n}$ and $\Phi_{\rm n}$ the equivalent input current and flux noise spectral density of the SQUID, respectively.

To quantify the maximum usable flux range of the SQUID, we need to realise that the output voltage and current of a SQUID is periodic modulo Φ_0 (the flux quantum) with respect to the input flux or current, and is typically close to sinusoidal. A sketch is shown in Fig. 1. For X-IFU we want to keep the bandwidth consumption low to minimise the power consumption, which implies that only the monotonic transfer range of the SQUID is usable. Fig. 1 shows the largest possible current/flux range (typically $\Phi_0/3$, 1.7 dB compression point), and a sketch of the linear range ($\Phi_0/18$, 0.04 dB compression point). When larger bandwidth consumption would be acceptable, multiple periods of the period response can be used, as shown by four-quadrant flux quanta counting [14], and by flux ramp modulation [15].

The rms flux noise of a SQUID depends on the bandwidth over which the noise is observed. So to match the signal dynamic range to a SQUID dynamic range requirement, the signal bandwidth needs to be specified as well. However, the nature of the calorimeter is such that the signal dynamic range is independent of the speed of the detector. Furthermore, the speed of the detector is not a fixed number, but is dependent on the chosen bias point and photon energy. Based on the science requirements, the micro-calorimeter designer chooses a certain combination of bias power level, T_c, and heat capacity[16]. As this translation from science requirements to micro-calorimeter parameters is not unique, we need to specify the readout requirements based on a chosen implementation, instead of basing it on the driving science requirements. It is therefore more convenient to define the dynamic range requirement of the pixels and their readout in terms of dynamic range *density* (DRD) instead of the dynamic range D. We define the DRD for a single pixel as

$$DRD_{\rm pix} \equiv \frac{\Delta I_{\rm max}}{i_{\rm ph}} = \frac{2\sqrt{2}I_0}{i_{\rm ph}} \frac{R_{\rm n} - R_0}{R_{\rm n}} = \sqrt{\frac{2P_0}{k_{\rm B}\gamma n T_{\rm c}}} \left(1 - \frac{R_0}{R_{\rm n}}\right), \qquad (1)$$

where the factor $2\sqrt{2}$ account for the amplitude ratio between the effective TES bias current, and the top-top value of a sinusoidal bias current, $i_{\rm ph}$ the phonon noise spectral density, n the exponent governing power flow through the heat link between the TES and the heat bath, γ a correction factor to account for the effects of nonlinear thermal conductance of the heat link on the phonon noise, $R_{\rm n}$ the normal state resistance of the TES, and R_0 the TES resistance in its setpoint, P_0 the operating power of the micro-calorimeter, and $T_{\rm c}$ the critical temperature of the TES. In summary, the $DRD_{\rm pix}$ can be described as the pixel dynamic range, normalised per unit bandwidth.

To translate this quantity into a dynamic range density requirement for the SQUID readout chain (DRD_{ro}) as part of a multiplexed channel, we need to include an error budget factor $F_b \equiv i_{\rm sq}/i_{\rm ph}$ with $i_{\rm ph}$ in the low frequency limit. Its value has been set at $F_b \approx 0.13$, which follows from the preliminary energy resolution budget. Furthermore, we need to include a factor accounting for the pile-up of X-ray photons. The TES bias currents at the input of SQUID are actively nulled by the baseband feedback, so that only photon absorptions in the detector pixels will induce flux excursions in the SQUID.

The latter property of FDM, in combination with the

science requirements, causes the SQUID DRD requirements ($DRD_{\rm sq}$) in a multiplexed channel to be virtually independent of the number multiplexed pixels under FDM for the X-IFU. This, in turn, is caused by the fact that the required $DRD_{\rm sq}$ in the SQUID depends on the probability of the occurrence of pile-up in a multiplexed channel with an amplitude larger than the largest amplitude of a signal in a single pixel. Because the effective area of the X-ray mirror decays with $\sim 1/E^2$ above $E \approx 2$ keV[1], and because the average count rate over the array is of the order of 2 counts/s, the probability of such an occurence is very low. This results in a monotonic DRD requirement for the SQUID in a channel with 40 multiplexed pixels of $DRD_{\rm sq} = F_b DRD_{\rm pix}$, without a multiplexing penalty.

IV. Minimisation of the SQUID power dissipation

To fit within the stringent power and mass budgets of the X-IFU instrument, the total dissipation of the front-end SQUIDs should be minimised, and should occur at the highest possible temperature.

The total power dissipation $P_{\rm tot}$ at the lowest temperature stage by the front-end SQUIDs can be written as

$$P_{\rm tot} = N_{\rm pix} P_{\rm sq} / N_{\rm mux}, \tag{2}$$

where $P_{\rm sq}$ is the power dissipation of a single front-end SQUID, $N_{\rm pix} = 3840$ the number of pixels, and $N_{\rm mux}$ the multiplex factor. $N_{\rm mux}$ needs to be maximised, and $P_{\rm sq}$ needs to be minimised to achieve the smallest heat load.

The achievable multiplex factor $N_{\rm mux}$ depends on the available bandwidth for multiplexing $B_{\rm mux}$, the inter pixel frequency spacing Δf as $N_{\rm mux} = B_{\rm mux}/\Delta f$, and the required dynamic range density of the readout chain $DRD_{\rm ro}$. In the two stage SQUID system, the value of $B_{\rm mux}$ is restricted by the interstage bandwidth $B_{\rm i}$, and by the bandwidth between the second stage SQUID and the room temperature amplifier. We restrict our discussion to the first regime, as in practical systems $B_{\rm i}$ has been shown to be limiting for $B_{\rm mux}$ [17], [6].

The value of $B_{\rm i}$ is set by the dynamic output resistance of the first stage SQUID $R_{\rm d1}$, and its inductive load consisting of the sum of the interstage cable inductance $L_{\rm c}$, and the input inductance $L_{\rm i2}$ of the second stage SQUID, so that $B_{\rm mux} = B_{\rm i} = R_{\rm d1}/2\pi(L_{\rm c} + L_{\rm i2})$.

The intrinsic dynamic range density of the a SQUID scales with its power dissipation $P_{\rm sq}$ as $DRD_{\rm sq} \propto \sqrt{P_{\rm sq}/k_{\rm B}T_{\rm sq}}$, with $T_{\rm sq}$ its operating temperature. Because the intrinsic DRD of an optimised state-of-the-art SQUID is significantly smaller than the required DRD in the readout chain, an independent baseband feedback loop per pixel[18], [19] has been baselined for the X-IFU. This electronics simultaneously provides the demodulation and carrier nulling functionality. The integrator in the forward path of a baseband feedback loop provides a loop gain $\mathscr{L}$ with an amplitude which is a function of frequency distance to the carrier frequency of a pixel, $f_{\rm n}$, following $\mathscr{L}(f - f_{\rm n}) \approx {\rm GBW}/|(f - f_{\rm n})|$ with GBW the gain times bandwidth which is approximately constant in a first order system with small propagation delay efffects.

In a baseband feedback system, there is an upper limit to the GBW in relation to the distance between the carrier frequencies $\Delta f = f_{\rm n} - f_{n-1}$, i.e. GBW $\lesssim \Delta f/6$. For an available multiplexing bandwidth $B_{\rm mux}$ we find GBW $\leq B_{\rm mux}/6N_{\rm mux}$[20].

As each baseband feedback loop exhibits classical flux locked loop [21], [22] behaviour, the net DRD of a SQUID chain with baseband feedback (DRD_{ro}) equals approximately $DRD_{ro} = DRD_{\rm sq}(1 + 2\pi\tau_{\rm r}{\rm GBW})$, with $\tau_{\rm r}$ the rise time of the X-ray responses.

Combining the relation between GBW and $B_{\rm mux}$ with the expression for DRD_{ro} in the applicable limit of $2\pi\tau_{\rm r}{\rm GBW} \gg 1$, we find that

$$N_{\rm mux} \propto \frac{2\pi\tau_{\rm r}\sqrt{P_{\rm sq}}}{\sqrt{P_0/k_{\rm B}T_{\rm c}}} B_{\rm i} \tag{3}$$

Before substituting this result in eq. (2), we need to establish the relation between $B_{\rm i}$ and $P_{\rm sq}$. Power dissipation in a SQUID scales as $P_{\rm sq} \propto \Delta I^2 R_{\rm d1}$. The output current swing capability ΔI is needed to drive the second stage SQUID over a sufficiently large flux range to match the dynamic range of the first stage SQUID. As shown earlier, $R_{\rm d1}$ provides interstage bandwidth dependent on the inductive load.

In the limit where the interstage cable inductance is small with respect to the input coil inductance of the second stage SQUID, i.e. $L_{\rm c} \ll L_{\rm i2}$, $B_{\rm i}$ is independent of $P_{\rm sq}$. This follows from the observation that a reduction of $P_{\rm sq}$ also reduces the intrinsic $DRD_{\rm sq}$ of the first stage SQUID, and therefore the required number of SQUID cells in the second stage array SQUID. This, in turn, reduces the required $L_{\rm i2}$ for a given flux range-ΔI combination so that the net value of $B_{\rm i}$ remains unchanged.

In the opposite limit, where the interstage cable inductance is dominant ($L_{\rm c} \gg L_{\rm i2}$), the inductive load of the first stage SQUID is independent of its power dissipation, so that $B_{\rm i} \propto P_{\rm sq}$ to maintain the intrinsic $DRD_{\rm sq}$ of the first stage SQUID.

We can now calculate the scaling of total power dissipation $P_{\rm tot}$ of the first stage SQUIDs with $P_{\rm sq}$, by combining eq. (2) and (3). For the two limits of the cable inductance we find

$$P_{\rm tot} \propto \begin{cases} N_{\rm pix}\frac{1}{2\pi\tau_{\rm r}}\sqrt{\frac{P_0}{k_{\rm B}T_{\rm c}}}\frac{1}{\sqrt{P_{\rm sq}}} & \text{if } L_{\rm c} \gg L_{\rm i2}. \\ N_{\rm pix}\frac{1}{2\pi\tau_{\rm r}}\sqrt{\frac{P_0}{k_{\rm B}T_{\rm c}}}\sqrt{P_{\rm sq}} & \text{if } L_{\rm c} \ll L_{\rm i2}. \end{cases} \tag{4}$$

This result leads to the conclusion that for a given value of $L_{\rm c}$ minimal total power dissipation is not obtained by minimising $P_{\rm sq}$, but by choosing $P_{\rm sq}$ such that $L_{\rm i2} \approx L_{\rm c}$ when the DRD of the first and second stage are matched. Although not clearly shown in this derivation, the lowest value of $P_{\rm tot}$ is found for the smallest value of $L_{\rm c}$.

Lowering $P_{\rm sq}$ below this optimum would decrease the multiplex factor $N_{\rm mux}$ more than proportional to $P_{\rm sq}$ both as a result of a smaller available multiplex bandwidth, and as a result of a smaller $DRD_{\rm sq}$. Increasing $P_{\rm sq}$ further would keep the available multiplex bandwidth remains fixed, so that the net multiplex factor only increases proportional to $\sqrt{P_{\rm sq}}$. This is a consequence of the fact that for a given $DRD_{\rm ro}$

TABLE I
SUMMARY OF THE REQUIRED SQUID PROPERTIES FOR THE X-IFU READOUT FOR A SINGLE READOUT CHAIN OF 40 PIXELS.

Property	**front-end SQUID**	**booster SQUID**
SQUID operating temperature $T_{\rm sq}$	50 mK	2 K
input inductance $L_{\rm in}$	< 3 nH	~ 80 nH
power dissipation $P_{\rm sq}$	< 2 nW	> 0.5 μW
equivalent input current noise $i_{\rm sq} = i_{\rm ph} F_{\rm b}$	< 3 pA/$\sqrt{\rm Hz}$	N/A
operating mode	single ended	differential
bandwidth 2-stage system	> 8 MHz	
interstage cable inductance $L_{\rm c}$	< 80 nH	
linearity 2-stage system	$< 1\%$ THD[a], (TBD)	

[a]Total Harmonic Distortion

requirement, it is more power effective to obtain DRD from a SQUID intrinsically, than from baseband feedback.

The resulting baselined SQUID tandem for the X-IFU consist of a multiloop front-end SQUID, and a large array SQUID as booster stage[17]. A summary of the properties is presented in table I.

V. OPTIMISATION OPTIONS

The first stage SQUID properties do not improve significantly below 300 mK, as a result of electron-phonon coupling limitations in the shunt resistors[23]. This implies that locating the first stage SQUIDs at the 300 mK level of the X-IFU would be sufficient to achieve full performance. A boundary condition for such a configuration is that the summing point inductance should be kept small, to avoid cross talk. Not only the first stage SQUIDs do not benefit from cooling below 300 mK, also the net impact of the Johnson noise of the equivalent series resistance in the capacitors of the LC filters is so low that its net effect on the detector performance will be $\sim 2\%$. Furthermore, the baselined design of the focal plane assembly (FPA)[2] is such that it will be relatively easy to thermally isolate the focal plane with the micro-calorimeter array from the LC filters and SQUIDs, because the flexible interconnects form a natural thermal barrier. This leads to the option to have the first stage SQUIDs at 300mK, so that a factor of ~ 10 larger power dissipation can be allowed, which would provide a lot of head room in the readout chain, and possibly a higher multiplex factor because the frequency space between pixels can be reduced when a lower GBW can be allowed because of the higher intrinsic dynamic range in the SQUIDs.

VI. ACKNOWLEDGEMENT

The research leading to these results has received funding from the European Unions Horizon 2020 Programme under the AHEAD project (grant agreement nr. 654215).

REFERENCES

[1] D. Barret, T. L. Trong, J.-W. den Herder, L. Piro, X. Barcons, J. Huovelin, R. Kelley, J. M. Mas-Hesse, K. Mitsuda, S. Paltani, G. Rauw, A. Rożanska, J. Wilms, M. Barbera, E. Bozzo, M. T. Ceballos, I. Charles, A. Decourchelle, R. den Hartog, J.-M. Duval, F. Fiore, F. Gatti, A. Goldwurm, B. Jackson, P. Jonker, C. Kilbourne, C. Macculi, M. Mendez, S. Molendi, P. Orleanski, F. Pajot, E. Pointecouteau, F. Porter, G. W. Pratt, D. Prêle, L. Ravera, E. Renotte, J. Schaye, K. Shinozaki, L. Valenziano, J. Vink, N. Webb, N. Yamasaki, F. Delcelier-Douchin, M. Le Du, J.-M. Mesnager, A. Pradines, G. Branduardi-Raymont, M. Dadina, A. Finoguenov, Y. Fukazawa, A. Janiuk, J. Miller, Y. Nazé, F. Nicastro, S. Sciortino, J. M. Torrejon, H. Geoffray, I. Hernandez, L. Luno, P. Peille, J. André, C. Daniel, C. Etcheverry, E. Gloaguen, J. Hassin, G. Hervet, I. Maussang, J. Moueza, A. Paillet, B. Vella, G. Campos Garrido, J.-C. Damery, C. Panem, J. Panh, S. Bandler, J.-M. Biffi, K. Boyce, A. Clénet, M. DiPirro, P. Jamotton, S. Lotti, D. Schwander, S. Smith, B.-J. van Leeuwen, H. van Weers, T. Brand, B. Cobo, T. Dauser, J. de Plaa, and E. Cucchetti, "The Athena X-ray Integral Field Unit (X-IFU)," *ArXiv e-prints*, Aug. 2016. [Online]. Available: https://arxiv.org/abs/1608.08105

[2] B. D. Jackson, H. van Weers, J. van der Kuur, R. den Hartog, H. Akamatsu, A. Argan, S. R. Bandler, M. Barbera, D. Barret, M. P. Bruijn, J. A. Chervenak, J. Dercksen, F. Gatti, L. Gottardi, D. Haas, J.-W. den Herder, C. A. Kilbourne, M. Kiviranta, T. Lam-Trong, B.-J. van Leeuwen, C. Macculi, L. Piro, and S. J. Smith, "The focal plane assembly for the athena x-ray integral field unit instrument," in *Proc. SPIE*, vol. 9905, 2016, pp. 99 052I–99 052I–8. [Online]. Available: http://dx.doi.org/10.1117/12.2232544

[3] T. Lam Trong, "X-ifu technical challenge," in *Proc. SPIE*, vol. 9905, 2016, pp. 99 052G–99 052G–17. [Online]. Available: http://dx.doi.org/10.1117/12.2233634

[4] I. Charles, C. Daniel, J. André, L. Duband, J.-M. Duval, R. den Hartog, K. Mitsuda, K. Shinozaki, H. van Weers, and N. Y. Yamasaki, "Preliminary thermal architecture of the x-ifu instrument dewar," in *Proc. SPIE*, vol. 9905, 2016, pp. 99 052J–99 052J–20. [Online]. Available: http://dx.doi.org/10.1117/12.2232710

[5] H. J. van Weers, J. W. den Herder, B. D. Jackson, P. P. K. Kooijman, C. Bruineman, K. Ravensberg, M. P. Bruijn, B. Rangarajan, A. J. van der Linden, M. L. Ridder, M. Leeman, B. J. van Leeuwen, A. Gotink, S. Kwast, T. J. van der Velde, J. R. H. Diesveld, C. Werner, and R. F. M. M. Hamelinck, "Tes-detector based focal plane assembly key-technology developments for athena and safari," in *Proc. SPIE*, vol. 9144, 2014, pp. 91 445R–91 445R–10. [Online]. Available: http://dx.doi.org/10.1117/12.2055454

[6] W. B. Doriese, K. M. Morgan, D. A. Bennett, E. V. Denison, C. P. Fitzgerald, J. W. Fowler, J. D. Gard, J. P. Hays-Wehle, G. C. Hilton, K. D. Irwin, Y. I. Joe, J. A. B. Mates, G. C. O'Neil, C. D. Reintsema, N. O. Robbins, D. R. Schmidt, D. S. Swetz, H. Tatsuno, L. R. Vale, and J. N. Ullom, "Developments in time-division multiplexing of x-ray transition-edge sensors," *Journal of Low Temperature Physics*, vol. 184, no. 1, pp. 389–395, 2016. [Online]. Available: http://dx.doi.org/10.1007/s10909-015-1373-z

[7] G. M. Stiehl, W. B. Doriese, J. W. Fowler, G. C. Hilton, K. D. Irwin, C. D. Reintsema, D. R. Schmidt, D. S. Swetz, J. N. Ullom, and L. R. Vale, "Code-division multiplexing for x-ray microcalorimeters," *Applied Physics Letters*, vol. 100, no. 7, 2012. [Online]. Available: http://scitation.aip.org/content/aip/journal/apl/100/7/10.1063/1.3684807

[8] J. van der Kuur, J. Beyer, M. Bruijn, J. Gao, R. den Hartog, R. Heijmering, H. Hoevers, B. Jackson, B. van Leeuwen, M. Lindeman, M. Kiviranta, P. de Korte, P. Mauskopf, P. de Korte, H. van Weers, and S. Withington, "The spica-safari tes bolometer readout: Developments towards a flight system," *J. Low Temp. Phys.*, vol. 167, pp. 561–567, 2012.

[9] K. Sakai, R. Yamamoto, Y. Takei, K. Mitsuda, N. Y. Yamasaki, M. Hidaka, S. Nagasawa, S. Kohjiro, and T. Miyazaki, "Development of frequency-division multiplexing readout system for large-format tes x-ray microcalorimeter arrays," *Journal of Low Temperature Physics*, vol. 184, no. 1, pp. 519–526, 2016. [Online]. Available: http://dx.doi.org/10.1007/s10909-016-1564-2

[10] M. A. Dobbs, M. Lueker, K. A. Aird, A. N. Bender, B. A. Benson, L. E. Bleem, J. E. Carlstrom, C. L. Chang, H.-M. Cho, J. Clarke, T. M. Crawford, A. T. Crites, D. I. Flanigan, T. de Haan, E. M. George, N. W. Halverson, W. L. Holzapfel, J. D. Hrubes, B. R. Johnson, J. Joseph, R. Keisler, J. Kennedy, Z. Kermish, T. M. Lanting, A. T. Lee, E. M. Leitch, D. Luong-Van, J. J. McMahon, J. Mehl, S. S. Meyer, T. E. Montroy, S. Padin, T. Plagge, C. Pryke, P. L. Richards, J. E. Ruhl, K. K. Schaffer, D. Schwan, E. Shirokoff, H. G. Spieler, Z. Staniszewski, A. A. Stark, K. Vanderlinde, J. D. Vieira,

C. Vu, B. Westbrook, and R. Williamson, "Frequency multiplexed superconducting quantum interference device readout of large bolometer arrays for cosmic microwave background measurements," *Review of Scientific Instruments*, vol. 83, no. 7, pp. –, 2012. [Online]. Available: http://scitation.aip.org/content/aip/journal/rsi/83/7/10.1063/1.4737629

[11] H. Akamatsu, L. Gottardi, J. van der Kuur, C. P. de Vries, K. Ravensberg, J. S. Adams, S. R. Bandler, M. P. Bruijn, J. A. Chervenak, C. A. Kilbourne, M. Kiviranta, A. J. van der Linden, B. D. Jackson, and S. J. Smith, "Development of frequency domain multiplexing for the x-ray integral field unit (x-ifu) on the athena," in *Proc. SPIE*, vol. 9905, 2016, pp. 99 055S–99 055S–8. [Online]. Available: http://dx.doi.org/10.1117/12.2232805

[12] J. van der Kuur, L. G. Gottardi, H. Akamatsu, B. J. van Leeuwen, R. den Hartog, D. Haas, M. Kiviranta, and B. J. Jackson, "Optimising the multiplex factor of the frequency domain multiplexed readout of the tes-based microcalorimeter imaging array for the x-ifu instrument on the athena x-ray observatory," in *Proc. SPIE*, vol. 9905, 2016, pp. 99 055R–99 055R–9, http://arxiv.org/abs/1611.05268. [Online]. Available: http://dx.doi.org/10.1117/12.2232830

[13] M. Kiviranta, L. Grönberg, and H. Sipola, "Two-stage locally linearized squid readout for frequency domain multiplexed calorimeter arrays," *Superconductor Science and Technology*, vol. 24, no. 4, p. 045003, 2011.

[14] M. Kiviranta and N. Beev, "Four-quadrant flux quanta counting for wide-range squid amplifiers," *Superconductor Science and Technology*, vol. 27, no. 7, p. 075005, 2014. [Online]. Available: http://stacks.iop.org/0953-2048/27/i=7/a=075005

[15] J. A. B. Mates, K. D. Irwin, L. R. Vale, G. C. Hilton, J. Gao, and K. W. Lehnert, "Flux-ramp modulation for squid multiplexing," *Journal of Low Temperature Physics*, vol. 167, no. 5, pp. 707–712, 2012. [Online]. Available: http://dx.doi.org/10.1007/s10909-012-0518-6

[16] S. J. Smith, J. S. Adams, S. R. Bandler, G. L. Betancourt-Martinez, J. A. Chervenak, M. P. Chiao, M. E. Eckart, F. M. Finkbeiner, R. L. Kelley, C. A. Kilbourne, A. R. Miniussi, F. S. Porter, J. E. Sadleir, K. Sakai, N. A. Wakeham, E. J. Wassell, W. Yoon, D. A. Bennett, W. B. Doriese, J. W. Fowler, G. C. Hilton, K. M. Morgan, C. G. Pappas, C. N. Reintsema, D. S. Swetz, J. N. Ullom, K. D. Irwin, H. Akamatsu, L. Gottardi, R. den Hartog, B. D. Jackson, J. van der Kuur, D. Barret, and P. Peille, "Transition-edge sensor pixel parameter design of the microcalorimeter array for the x-ray integral field unit on athena," in *Proc. SPIE*, vol. 9905, 2016, pp. 99 052H–99 052H–19. [Online]. Available: http://dx.doi.org/10.1117/12.2231749

[17] M. Kiviranta, L. Grönberg, N. Beev, and J. van der Kuur, "Some phenomena due to squid input properties when local feedback is present," *Journal of Physics: Conference Series*, vol. 507, no. 4, p. 042017, 2014. [Online]. Available: http://stacks.iop.org/1742-6596/507/i=4/a=042017

[18] M. Kiviranta, H. Seppä, J. van der Kuur, and P. de Korte, "SQUID-based readout schemes for microcalorimeter arrays," in *AIP Conference Proceedings LTD-9*, F. Porter, D. McCammon, M. Galeazzi, and C. Stahle, Eds., vol. 605. AIP, 2002, pp. 295–300.

[19] L. Ravera, C. Cara, M. T. Ceballos, X. Barcons, D. Barret, R. Cldassou, A. Clnet, B. Cobo, E. Doumayrou, R. H. den Hartog, B.-J. van Leeuwen, D. van Loon, J. M. Mas-Hesse, C. Pigot, and E. Pointecouteau, "The dre: the digital readout electronics for athena x-ifu," in *Proc. SPIE*, vol. 9144, 2014, pp. 91 445T–91 445T–8. [Online]. Available: http://dx.doi.org/10.1117/12.2055750

[20] R. den Hartog, D. Boersma, M. Bruijn, B. Dirks, L. Gottardi, H. Hoevers, R. Hou, M. Kiviranta, P. de Korte, J. van der Kuur, B. van Leeuwen, A. Nieuwenhuizen, and M. Popescu, "Baseband feedback for frequencydomainmultiplexed readout of tes xray detectors," *AIP Conference Proceedings*, vol. 1185, no. 1, pp. 261–264, 2009. [Online]. Available: http://scitation.aip.org/content/aip/proceeding/aipcp/10.1063/1.3292328

[21] J. Clarke, "Squid fundamentals," in *SQUID sensors: fundamentals, fabrication and applications*, ser. NATO ASI series E: Applied sciences 329, H. Weinstock, Ed. Dordtrecht, the Netherlands: Kluwer Academic, 1996, pp. 1–62.

[22] F. Wellstood, C. Heiden, and J. Clarke, "Integrated dc squid magnetometer with a high slew rate," *Rev. Sci. Instrum.*, vol. 55, no. 6, p. 952, 1984.

[23] M. Kiviranta, J. S. Penttila, L. Grönberg, H. Seppä, and I. Suni, "Dc- and un-squids for readout of ac-biased transition-edge sensors," *IEEE Transactions on Applied Superconductivity*, vol. 13, no. 2, pp. 614–617, June 2003.